511

Copy
RM E58G02

NACA RM E58G02

NACA

RESEARCH MEMORANDUM

EXPERIMENTAL INVESTIGATION OF EFFECT OF SPIKE-TIP AND COWL-LIP BLUNTING ON THE INTERNAL PERFORMANCE OF A TWO-CONE CYLINDRICAL-COWL INLET AT MACH NUMBER 4.95

By Kenneth C. Weston

Lewis Flight Propulsion Laboratory
Cleveland, Ohio

CLASSIFICATION CHANGED
TO [redacted]
By Authority of TP 71-242 Date 330-7

N71-72112
(ACCESSION NUMBER) (THRU)
15 None
(PAGES) (CODE)
(NASA CR OR TMX OR AD NUMBER) (CATEGORY)
FACILITY FORM 602

NATIONAL ADVISORY COMMITTEE
FOR AERONAUTICS
WASHINGTON

September 23, 1958

CONFIDENTIAL

[redacted]

NATIONAL ADVISORY COMMITTEE FOR AERONAUTICS

RESEARCH MEMORANDUM

EXPERIMENTAL INVESTIGATION OF EFFECT OF SPIKE-TIP AND COWL-LIP BLUNTING ON THE INTERNAL PERFORMANCE OF A TWO-CONE CYLINDRICAL-COWL INLET AT MACH NUMBER 4.95*

By Kenneth C. Weston

SUMMARY

The effect of blunting on the internal performance of a two-cone inlet with an internally cylindrical cowl was investigated experimentally at a Mach number of 4.95. Cowl-lip blunting resulted in increases in peak pressure recovery (approximately $1\frac{1}{2}$ counts) and critical mass-flow ratio (approximately 3 counts), but the mass-flow increases are apparently the result of the spike shock spillage of all configurations. Decreases in both peak total-pressure recovery and critical mass flow resulted from spike-tip blunting. Wave drag due to blunting is estimated.

INTRODUCTION

Considerable research has been done in the supersonic inlet field below flight Mach numbers of 4. This research has, in general, been concerned with the use of sharp spike tips and cowl lips, with the exception of a few investigations directed primarily at improvement of supersonic inlet performance at subsonic speeds (for instance, ref. 1). The use of sharp leading edges at the low supersonic Mach numbers has been relatively unchallenged because of the large drag penalties and local total-pressure losses associated with a bow wave produced by blunting.

Consideration of the aerodynamic heating of sharp slender bodies in the hypersonic speed range, however, quickly leads to the conclusion that the structural integrity of the leading edges of such bodies is at best difficult to maintain. It is well known that the leading-edge heating problem can be relieved by blunting; stagnation-point heating rates decrease as the inverse square root of the radius of blunting, and the total tip heat transfer is reduced accordingly.

In relieving the heating problems through blunting, it is expected that internal performance may be sacrificed and drag increased. The

[redacted]

obvious effect of blunting is the total-pressure loss suffered by the stream tube traversing the shock wave in the stagnation region. Because of the curvature of the bow shock, the total-pressure loss varies from normal-shock value along the stagnation streamline to cone or wedge value at distances large compared with the radius of blunting. As a result, a layer of low-total-pressure air adjacent to the body surface is formed, known as the inviscid shear layer (described and analyzed in ref. 2). Reference 2 indicates that friction and heat-transfer characteristics may be influenced to a considerable extent by the shear layer. It is likely that, for the inlet application, the shear layer may play a significant role in interactions with compression surface and diffuser adverse pressure gradients. It appears that these interactions would be detrimental to inlet performance. While cowl pressure drag increases with blunting, some reduction in cowl friction drag may be obtained because of the influence of blunting on boundary-layer transition.

In order to evaluate the effects of blunting on internal performance in the hypersonic range, a test program was initiated and run in the Lewis laboratory variable Reynolds number jet at a Mach number of 4.95. Total-pressure-recovery and mass-flow data were obtained for a range of spike and cowl bluntnesses. Actual drags were not measured, but the magnitude of the drag due to blunting is estimated.

An investigation of the effects of blunting (including drag measurements) on inlet performance at a Mach number of 3.0 was conducted simultaneously with the present tests and is reported in reference 3.

SYMBOLS

A	area
$C_{D,b}$	drag coefficient due to blunting
C_p	pressure coefficient
M	Mach number
m	mass-flow rate
m_0	reference mass-flow rate, based on area $\pi(R_i + r_c)^2$
m/m_0	mass-flow ratio
P	total pressure
P/P_0	total-pressure ratio

5060

CI-1 back

p	static pressure
q	dynamic pressure
R_c	cowl radius (defined in fig. 6)
R_i	internal cowl radius, 1.799 in.
r_c	radius of cowl blunting (defined in fig. 6)
r_s	radius of spike blunting
S	surface area
θ	angle (defined in fig. 6)
θ_N	nacelle angle

Subscripts:

t	stagnation value
0	free-stream conditions

APPARATUS AND PROCEDURE

Inlet Geometry

In order to determine the effects of blunting on internal inlet performance, a two-cone fixed-geometry comparison inlet with an internally cylindrical cowl was designed for a free-stream Mach number of 4.95. It is recognized that other inlet types, particularly those employing variable geometry, may provide significantly higher pressure recoveries than the inlet selected. Nevertheless, the complications implicit in variable geometry at high Mach numbers make the simplicity of the fixed-geometry inlet attractive, at least in the early development of hypersonic engines (ref. 4). The comparison inlet was designed with a low-drag cowl (similar to that of ref. 5) and employed sharp leading edges. The cone angles were selected as those giving maximum total-pressure recovery consistent with the requirement that the internally cylindrical cowl deflect the compressed flow field through an angle of approximately 4° less than that for shock detachment. These cone angles were a 20° half-cone angle followed by a 12° increase in angle. Centerbody and cowl coordinates are given in figure 1.

Three flush centerbody boundary-layer-bleed slots were located in the throat in the vicinity of the shoulder. These slots are designated

[redacted]

A, B, and C. Equally spaced holes were drilled at the bottom of the slots connecting with the centerbody interior. Bleed air was ducted through the centerbody and out through three centerbody support struts of the existing model support system (see fig. 2), which were vented to free-stream static pressure. Bleed-slot locations are given in figure 1. All data presented here were obtained with slots B and C filled and smoothed.

The comparison inlet allowed interchanging the blunted and sharp cowls with no change in the internal flow passage (except at the cowl lip). All cowls were designed so that their free-stream stagnation points were in the same axial plane relative to the centerbody. This is illustrated in figure 1 by the cowls designated 2 and 3.

The comparison inlet also incorporated a removable first cone that could be replaced by blunted cones. These cones were identical except in the blunted spherical tips, which were tangent to the 40°-included-angle cone surface. These cones are designated 2 and 3 in order of increasing blunting. All tests were run with the same effective tip projection (except those shown in fig. 3(b)); that is, the spike tips were changed without changing the relative position of the centerbody and cowl. Figure 1 shows the ratios of the spike and cowl bluntness radius to the internal cowl radius (1.799 in.).

Experimental Procedure

The arithmetic mean of the pressures obtained from an area-weighted rake was taken as the diffuser-exit total pressure. The mass-flow ratio was calculated by using a calibrated choked plug and the total-pressure recovery assuming no change in total pressure between rake and plug. It should be noted that the ideal capture area was calculated using a capture radius composed of the sum of the internal cowl radius (R_i) and the radius of blunting (r_c). Thus, equal mass-flow ratios with different cowls would result in different mass flows for each configuration.

The experimental tests were conducted in the NACA Lewis variable Reynolds number jet at a Mach number of 4.95 and a simulated pressure altitude of approximately 88,000 feet (with the exception of one run shown in fig. 3(a)). The tunnel total temperature was maintained at 250° ±10° F, and the dewpoint at approximately -70° F. The test Reynolds number was 1.66×10^6 based on reference inlet capture diameter of 3.598 inches.

PERFORMANCE OF COMPARISON INLET

The comparison inlet was designed with a cylindrical cowl to turn the internal flow through a shock wave in a manner similar to the inlet reported in reference 5. It was indicated there that bleed in the inlet

throat in the vicinity of the centerbody shoulder was necessary to achieve attachment of the internal cowl shock at a Mach number of 2.95. This was not true for the present case (sharp spike and cowl) at Mach 4.95. No combination of throat bleed slots or single slot was sufficient for shock attachment. The ineffectiveness of the throat bleed is probably the result of the more severe pressure gradient of the internal cowl shock wave due to the higher free-stream Mach number. The static-pressure ratio across the cowl-generated shock for the comparison inlet is calculated to be about 5.0 near the cowl, while a value of 2.9 was obtained for the inlets of reference 5. No bleed variations were tested in conjunction with the blunted leading edges.

The effect of Reynolds number on performance of the comparison inlet is shown in figure 3(a). The higher unit Reynolds number results in higher peak pressure recovery and supercritical mass-flow ratios than the lower Reynolds number. Inspection of the accompanying schlieren photographs indicates that this is indeed a boundary-layer phenomenon. At the lower unit Reynolds number, the boundary-layer separation bridging the junction of the first and second cones is enlarged. This results in forward movement of the shock wave at the separation point so that it intersects the first cone shock ahead of the cowl. Such modifications of the cowl shock can result in significant mass-flow losses, as witnessed by the large combined spillage and bleed mass-flow ratios $(1 - m/m_0)$. The decreased pressure recovery is not so easily explained, but it appears to be intimately associated with the thickening of the spike junction separation. Because of these changes of inlet performance with the change in unit Reynolds number, it is apparent that the spike boundary layer must be carefully considered in inlet design in the hypersonic regime.

The effect of variation of spike-tip projection on sharp-inlet performance is shown in figure 3(b). Increasing spike-tip projection resulted in decreases in both critical mass-flow ratio and peak pressure recovery. Design tip projection is 3.840 inches.

EFFECT OF BLUNTING

Blunt-Inlet Performance

The spike tip of the comparison inlet can be replaced by a blunted spike without changing the inlet in any other respect. Figure 4(a) shows comparison-inlet performance as affected by spike blunting. Spike blunting resulted in decreased pressure recovery and supercritical mass-flow ratio. The decrease in mass-flow ratio is presumably the result of an increase in the slope of the initial shock in the vicinity of the cowl lip. This change in the shock may be attributed to disturbances arising from the combined interaction of shear layer, compression-surface boundary layer, and initial conical flow field.

[redacted]

The variation of inlet performance with spike-tip blunting when the blunted cowls are used is given in figures 4(b) and (c). The same trend with spike blunting is apparent with the blunted cowls as with the sharp cowl. Large performance decrements are observed in all cases when spike 1 is replaced by spike 2. Additional blunting (spike 3) resulted in little further change in inlet performance. Evidently, further spike blunting must eventually have a more pronounced effect on inlet performance. This was observed with a spike ($r_s/R_i = 0.150$) blunter than spike 3 in conjunction with the blunted cowls. Unsteady flow and very poor pressure recoveries were obtained in these cases (data not presented).

The data of figure 4 are rearranged in figure 5 to show the effect of cowl blunting on inlet performance. Figure 5(a) shows pressure-recovery - mass-flow-ratio results when the cowl of the comparison inlet is replaced by blunted cowls. Cowl blunting resulted in both increased total-pressure recovery and mass-flow ratio. The variation of mass-flow ratio with cowl bluntness radius depends on the manner in which the cowl is blunted, on the reference area chosen, and on the relative position of cowl lip to the shocks from the compression surface. In the present tests the family of blunted cowls was selected so that the spike-tip projection (for a given spike) has a constant value. The reference area was selected as that corresponding to the radius $R_i + r_c$, since this gives maximum mass-flow ratios of unity with the tip shock inside the cowl and, furthermore, reduces to the usual definition of capture area with a zero radius of blunting (sharp lip). Because of the complexity of the flow field at the cowl lip, it is difficult to ascertain the reason for the increase in mass flow with increase in blunting. As a check, a two-dimensional calculation was made based on a flow model that presumably simulated the spike shock spillage near the cowl lip. This calculation is in qualitative agreement with the observed mass-flow increases. The increases in mass-flow ratio would of course be impossible if the sharp inlet had captured a full stream tube.

Figures 5(b) and (c) show the effect of cowl blunting on inlet performance with spikes 2 and 3, respectively. The trend of performance with the sharp spike is reaffirmed here with the blunted spikes.

Estimate of Drag Due to Blunting

No force measurements were made in the present tests, but it is of interest to estimate the drag associated with cowl blunting. An estimate can be readily made of the incremental wave drag coefficient due to blunting for the simplified case of external shocks falling inside the cowl so that the cowl-lip pressure distribution is well represented by the Newtonian pressure distribution. Details of the calculation are presented in the appendix, and the results in the form of wave drag coefficient due to blunting are plotted against bluntness radius ratio in

figure 6. The figure shows, for example, that a 4-foot-diameter engine with a 0.935-inch cowl bluntness radius can have an incremental drag coefficient due to blunting of 0.10 at Mach 5.0. At higher flight Mach numbers the bluntness drag coefficient increases only slightly, but percentagewise the drag is much more significant in terms of net thrust because of the decrease of engine thrust coefficients with increasing Mach number. However, reduction in friction drag due to longer runs of laminar boundary layer may be obtained by cowl blunting.

SUMMARY OF RESULTS

An experimental investigation of the effects of blunting on the performance of a two-cone inlet with an internally cylindrical cowl at a Mach number of 4.95 may be summarized as follows:

1. Spike-tip blunting resulted in reductions in peak total-pressure recovery and mass-flow ratio.

2. Cowl blunting resulted in increases in peak total-pressure recovery and supercritical mass-flow ratio, but the mass-flow effect is apparently the result of spike shock spillage.

Lewis Flight Propulsion Laboratory
National Advisory Committee for Aeronautics
Cleveland, Ohio, July 10, 1958

[redacted]

APPENDIX - CALCULATION OF INCREMENTAL DRAG COEFFICIENT DUE TO BLUNTING

The incremental drag coefficient due to bluntness shown in figure 6 is obtained by integrating the Newtonian pressure distribution, neglecting the centrifugal correction, over a toroidal area from the stagnation point. From the definition of pressure-drag coefficient,

$$C_{D,b} = \frac{1}{q_0 A_0} \int_S (p - p_0) \cos \theta \, dS$$

and the Newtonian distribution,

$$C_p = C_{p,t} \cos^2\theta$$

the following integral is obtained for the bluntness drag coefficient:

$$C_{D,b} = \frac{2\pi r_c C_{p,t}}{A_0} \int_0^{\theta_N} \cos^3\theta (R_c + r_c \sin \theta) d\theta$$

Evaluation of the integral and expression of A_0 in terms of R_c gives the following expression for $C_{D,b}$ in terms of bluntness radius ratio and θ_N:

$$C_{D,b} = 2C_{p,t}\left[\frac{r_c}{R_c} \sin \theta_N - \frac{1}{3}\left(\frac{r_c}{R_c}\right)\sin^3\theta_N - \frac{1}{4}\left(\frac{r_c}{R_c}\right)^2\left(\cos^4\theta_N - 1\right)\right]$$

For $\theta_N = \pi/2$ (i.e., a zero external angle cowl),

$$C_{D,b} = C_{p,t}\left[\frac{4}{3}\left(\frac{r_c}{R_c}\right) + \frac{1}{2}\left(\frac{r_c}{R_c}\right)^2\right]$$

This relation applies only when the cowl lip is free of the interference field formed by the inlet centerbody; that is, the spike shock must be inside the inlet. Interference of the centerbody flow field with the cowl shock causes a decrease in the area of the maximum capture stream tube as well as surface pressure changes. These effects will result in higher drag coefficients than those indicated.

The stagnation-pressure coefficients used in figure 6 were calculated for air in thermodynamic equilibrium with the method of reference 6 and the thermodynamic property charts of reference 7.

[redacted]

REFERENCES

1. Gorton, Gerald C., and Dryer, Murray: Comparison at Supersonic Speeds of Translating Spike Inlets Having Blunt- and Sharp-Lip Cowls. NACA RM E54J07, 1955.

2. Moeckel, W. E.: Some Effects of Bluntness on Boundary-Layer Transition and Heat Transfer at Supersonic Speeds. NACA Rep. 1312, 1957. (Supersedes NACA TN 3653.)

3. Cubbison, R. W., and Samanich, N. E.: Effect of Spike-Tip and Cowl-Lip Blunting on Inlet Performance of a Mach 3.0 External-Compression Inlet. NACA RM E58G02a, 1958.

4. Connors, James F., and Allen, John L.: Survey of Supersonic Inlets for High Mach Number Applications. NACA RM E58A20, 1958.

5. Weston, Kenneth C., and Kowalski, Kenneth L.: Experimental Investigation of Extreme Internal Flow Turning at the Cowl Lip of an Axisymmetric Inlet at a Mach Number of 2.95. NACA RM E58A27a, 1958.

6. Moeckel, W. E.: Oblique-Shock Relations at Hypersonic Speeds for Air in Chemical Equilibrium. NACA TN 3895, 1957.

7. Moeckel, W. E., and Weston, Kenneth C.: Composition and Thermodynamic Properties of Air in Chemical Equilibrium. NACA TN 4265, 1958.

5060

CI-2

[redacted]

5060

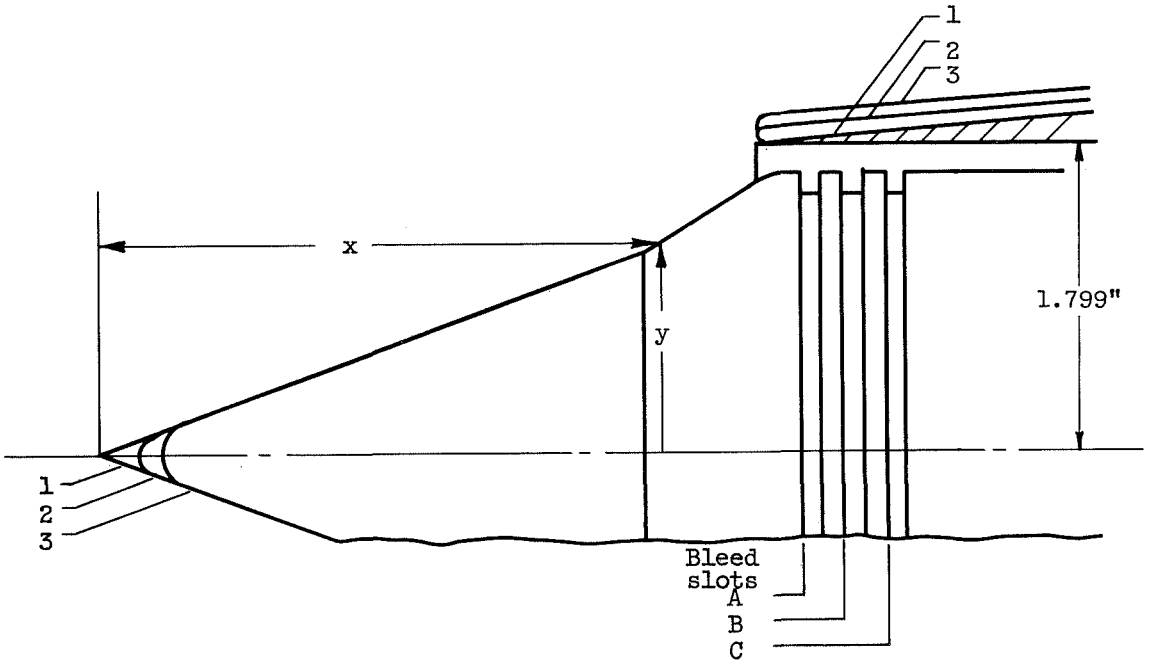

Reference inlet centerbody coordinates	
x	y
0	0
3.210	1.168
3.906	1.603
3.950	1.620
4.000	1.627
5.500	1.627
6.000	1.618
7.000	1.580
8.000	1.542
9.000	1.492
10.000	1.430
11.000	1.378
12.000	1.320

Spike bluntness radius	
Spike designation	r_s/R_i
1 (sharp)	0.001
2	.070
3	.111

Cowl bluntness radius	
Cowl designation	r_c/R_i
1 (sharp)	0.001
2	.011
3	.027

Bleed slot coordinates	
Slot	Distance to leading edge, in.
A	4.094
B	4.344
C	4.594

Figure 1. - Schematic diagram of supersonic inlet with pertinent dimensions.

5060
CI-2 back

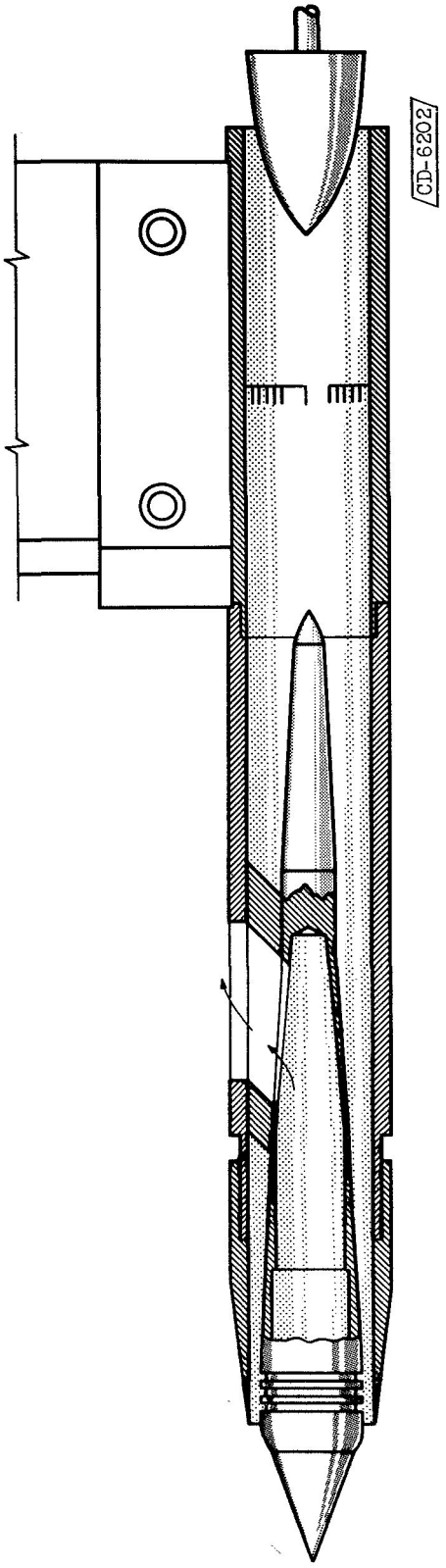

Figure 2. - Supersonic inlet and model support system.

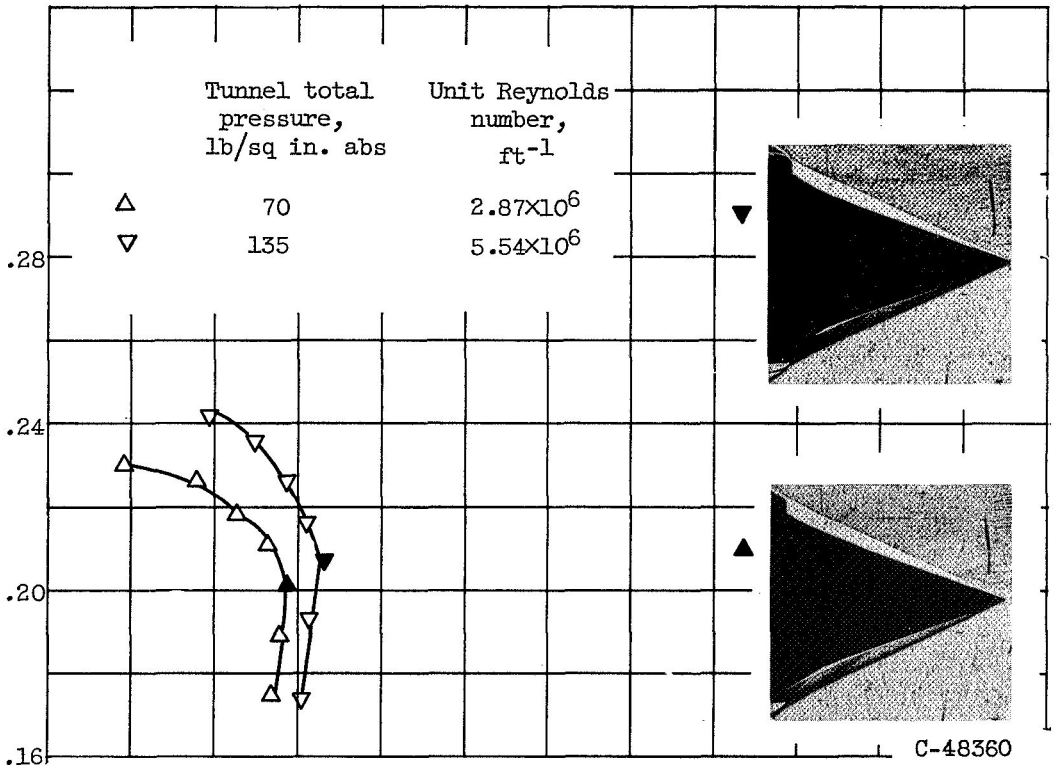

(a) Effect of tunnel total pressure on inlet performance. Tip projection, 3.855 inches.

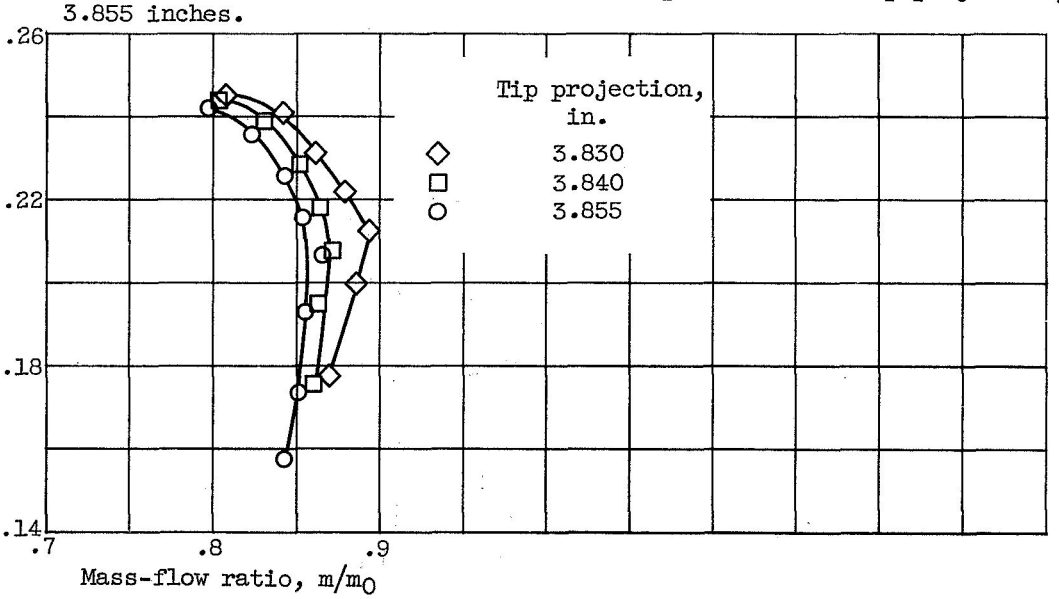

Total-pressure recovery, P/P_0

(b) Effect of tip projection on inlet performance. Sharp spike and cowl.

Figure 3. - Reference inlet performance. Free-stream Mach number, 4.95; slot A open.

5060

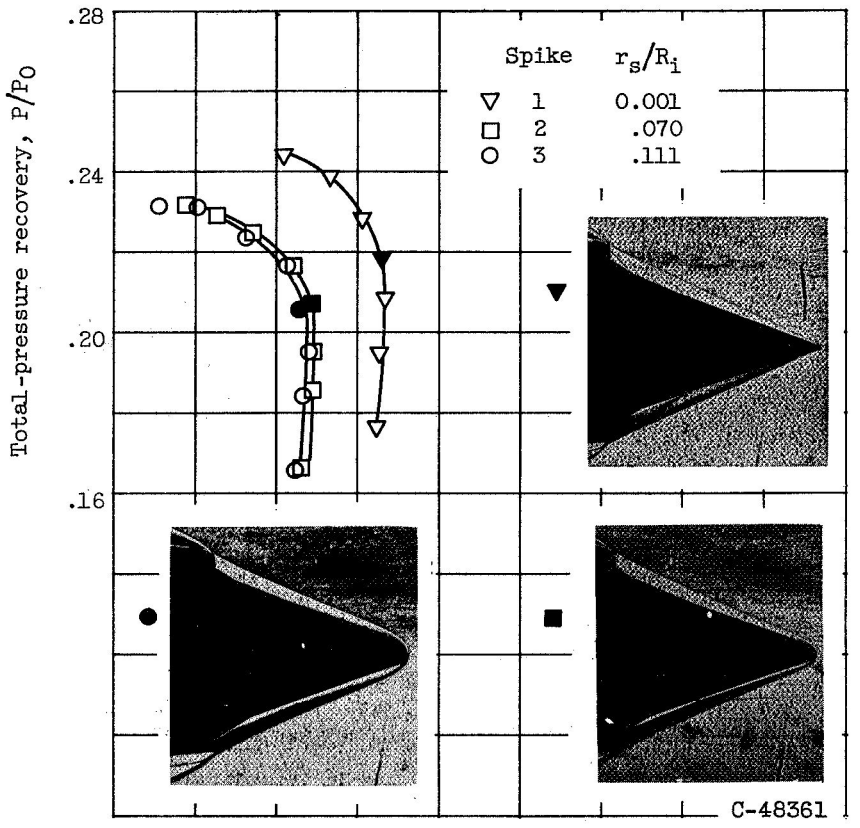

(a) Cowl 1 (sharp).

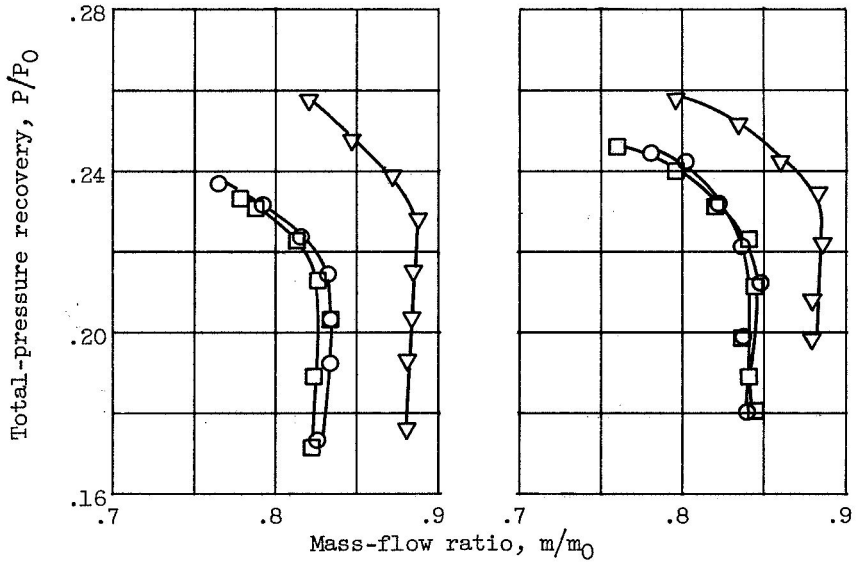

(b) Cowl 2. (c) Cowl 3.

Figure 4. - Effect of spike blunting on inlet performance. Free-stream Mach number, 4.95; slot A open; equivalent tip projections.

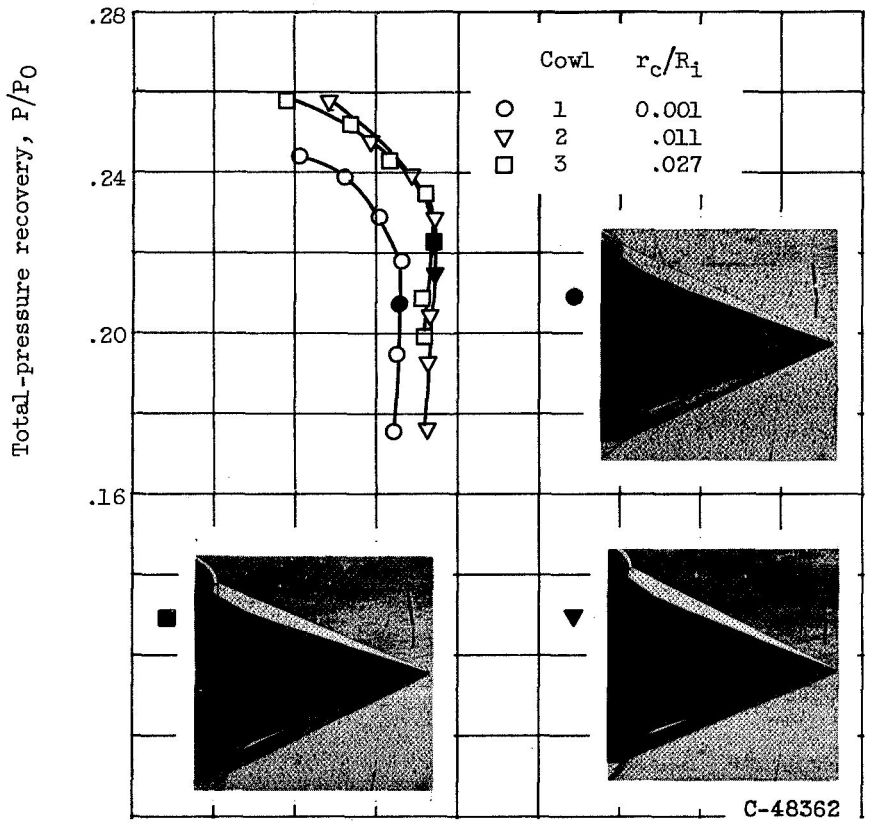

(a) Spike 1 (sharp).

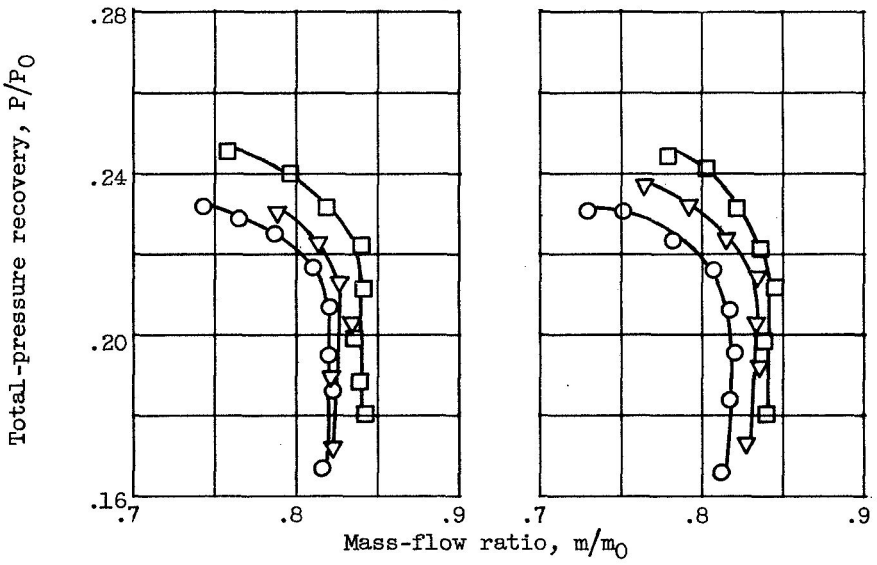

(b) Spike 2. (c) Spike 3.

Figure 5. - Effect of cowl blunting on inlet performance. Free-stream Mach number, 4.95; slot A open; tip projection, 3.84 inches.

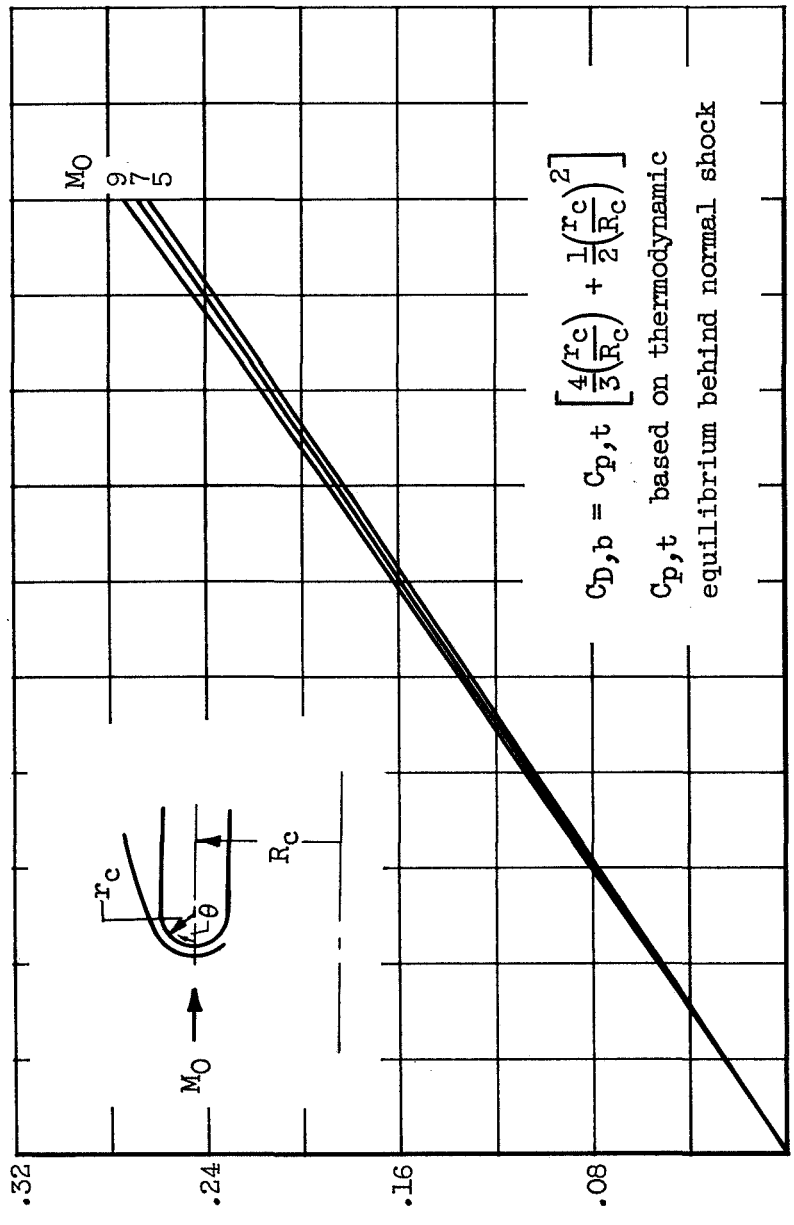

Figure 6. - Effect of cowl blunting on incremental wave drag coefficient due to blunting.

NOTES: (1) Reynolds number is based on the diameter of a circle with the same area as that of the capture area of the inlet.

(2) The symbol * denotes the occurrence of buzz.

CONFIDENTIAL

INLET BIBLIOGRAPHY SHEET

Report and facility	Description			Test parameters				Test data				Performance		Remarks
	Configuration	Number of oblique shocks	Type of boundary-layer control	Free-stream Mach number	Reynolds number $\times 10^{-6}$	Angle of attack, deg	Angle of yaw, deg	Drag	Inlet-flow profile	Discharge-flow profile	Flow picture	Maximum total-pressure recovery	Mass-flow ratio	
CONFID. RM E58G02 Variable Reynolds number jet	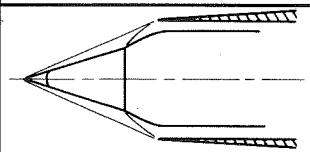 Fixed-geometry, two-cone inlet	3	Flush slots in throat	4.95	1.66	0	0				√	25.8	0.73*-0.89	The effect of cowl-lip and spike-tip blunting on inlet performance was determined.
CONFID. RM E58G02 Variable Reynolds number jet	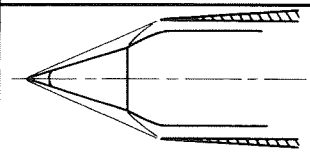 Fixed-geometry, two-cone inlet	3	Flush slots in throat	4.95	1.66	0	0				√	25.8	0.73*-0.89	The effect of cowl-lip and spike-tip blunting on inlet performance was determined.
CONFID. RM E58G02 Variable Reynolds number jet	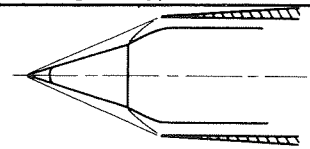 Fixed-geometry, two-cone inlet	3	Flush slots in throat	4.95	1.66	0	0				√	25.8	0.73*-0.89	The effect of cowl-lip and spike-tip blunting on inlet performance was determined.
CONFID. RM E58G02 Variable Reynolds number jet	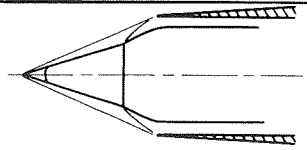 Fixed-geometry, two-cone inlet	3	Flush slots in throat	4.95	1.66	0	0				√	25.8	0.73*-0.89	The effect of cowl-lip and spike-tip blunting on inlet performance was determined.

Bibliography

These strips are provided for the convenience of the reader and can be removed from this report to compile a bibliography of NACA inlet reports. This page is being added only to inlet reports and is on a trial basis.

CONFIDENTIAL